

Dale, Jonathan, Cundy, Andrew B., Spencer, Kate L., Carr, Simon ORCID: <https://orcid.org/0000-0003-4487-3551> , Croudace, Ian W., Burgess, Heidi M. and Nash, David J. (2019) Sediment structure and physicochemical changes following tidal inundation at a large open coast managed realignment site. *Science of the Total Environment*, 660 . pp. 1419-1432.

Downloaded from: <http://insight.cumbria.ac.uk/id/eprint/4528/>

Usage of any items from the University of Cumbria's institutional repository 'Insight' must conform to the following fair usage guidelines.

Any item and its associated metadata held in the University of Cumbria's institutional repository Insight (unless stated otherwise on the metadata record) may be copied, displayed or performed, and stored in line with the JISC fair dealing guidelines (available [here](#)) for educational and not-for-profit activities

provided that

- the authors, title and full bibliographic details of the item are cited clearly when any part of the work is referred to verbally or in the written form
 - a hyperlink/URL to the original Insight record of that item is included in any citations of the work
- the content is not changed in any way
- all files required for usage of the item are kept together with the main item file.

You may not

- sell any part of an item
- refer to any part of an item without citation
- amend any item or contextualise it in a way that will impugn the creator's reputation
- remove or alter the copyright statement on an item.

The full policy can be found [here](#).

Alternatively contact the University of Cumbria Repository Editor by emailing insight@cumbria.ac.uk.

1 **Sediment structure and physicochemical changes following tidal inundation**
2 **at a large open coast managed realignment site**

3 Jonathan J. Dale^{1,2*}, Andrew B. Cundy³, Kate L. Spencer⁴, Simon J. Carr^{4,5}, Ian W. Croudace³,
4 Heidi M. Burgess¹ and David J. Nash^{1,6}

5 ¹Centre for Aquatic Environments, School of Environment and Technology, University of
6 Brighton, Brighton, BN2 4GJ, UK.

7 ²School of Energy, Construction and Environment, Coventry University, Coventry CV1 5FB,
8 UK.

9 ³School of Ocean and Earth Science, University of Southampton, National Oceanography
10 Centre (Southampton), Southampton, SO14 3ZH, UK.

11 ⁴School of Geography, Queen Mary University of London, London, E1 4NS.

12 ⁵Science, Natural Resources & Outdoor Studies, University of Cumbria, Rydal Road,
13 Ambleside, Cumbria LA22 9BB, U.K.

14 ⁶School of Geography, Archaeology and Environmental Studies, University of the
15 Witwatersrand, Private Bag 3, Wits 2050, South Africa.

16

17 ***Corresponding Author:**

18 Jonathan Dale

19 School of Environment and Technology, University of Brighton, Cockcroft Building, Lewes
20 Road, Brighton, UK, BN2 4GJ. Email: J.J.Dale@brighton.ac.uk

21

22 **Published in Science of the Total Environment, Volume 660, pp 1419-1432,**
23 **2019.**

24 **Authors' pre-print version**

25

26 **Keywords**

27 Managed realignment; Microtomography; Sediment Structure; Saltmarsh Geochemistry;

28 Itrax XRF

29

30 **1 Abstract**

31

32 Managed realignment (MR) schemes are being implemented to compensate for the loss of
33 intertidal saltmarsh habitats by breaching flood defences and inundating the formerly
34 defended coastal hinterland. However, studies have shown that MR sites have lower
35 biodiversity than anticipated, which has been linked with anoxia and poor drainage resulting
36 from compaction and the collapse of sediment pore space caused by the site's former
37 terrestrial land use. Despite this proposed link between biodiversity and soil structure, the
38 evolution of the sediment sub-surface following site inundation has rarely been examined,
39 particularly over the early stages of the terrestrial to marine or estuarine transition. This
40 paper presents a novel combination of broad- and intensive-scale analysis of the sub-
41 surface evolution of the Medmerry Managed Realignment Site (West Sussex, UK) in the
42 three years following site inundation. Repeated broad-scale sediment physiochemical
43 datasets are analysed to assess the early changes in the sediment subsurface and the
44 preservation of the former terrestrial surface, comparing four locations of different former
45 land uses. Additionally, for two of these locations, high-intensity 3D-computed X-ray
46 microtomography and Itrax micro-X-ray fluorescence spectrometry analyses are presented.
47 Results provide new data on differences in sediment properties and structure related to the
48 former land use, indicating that increased agricultural activity leads to increased compaction
49 and reduced porosity. The presence of anoxic conditions, indicative of poor hydrological
50 connectivity between the terrestrial and post-inundation intertidal sediment facies, was
51 only detected at one site. This site has experienced the highest rate of accretion over the
52 terrestrial surface (*ca.* 7 cm over 36 months), suggesting that poor drainage is caused by the

53 interaction (or lack of) between sediment facies rather than the former land use. This has
54 significant implications for the design of future MR sites in terms of preparing sites, their
55 anticipated evolution, and the delivery of ecosystem services.

56

57

58 **2 Introduction**

59

60 Saltmarsh and mudflat environments provide a range of ecosystem services (Costanza et al.,
61 1997) including detoxification, nursery habitat and flood defence through the attenuation of
62 wave energy (e.g. Moller et al., 2014; Rupprecht et al., 2017). However, these habitats are
63 threatened by sea level rise, causing erosion and coastal squeeze (e.g. Doody, 2004), and
64 anthropogenic pressures including pollution and reclamation in response to urbanisation
65 and population growth. This has resulted in the loss and degradation of coastal habitats
66 worldwide. In recent years, there have been a number of schemes implemented to
67 compensate for these losses, frequently driven by legislative requirements to improve
68 habitats and biodiversity such as the EU Habitats Directive (European Parliament and the
69 Council of the European Commission, 1992). These schemes use ecological engineering (or
70 ecoengineering) approaches (Bergen et al., 2001) and aim to restore the structure and
71 function of intertidal environments, either through habitat creation or by engineering
72 physical processes to create the desired conditions to encourage habitat creation (Elliott et
73 al., 2016). This paper focuses on managed realignment (MR), one of the most popular
74 coastal ecoengineering techniques.

75

76 MR describes the practice of inundating areas of the coastal hinterland through de-
77 embanking, removing or breaching the former flood defences, with new defences
78 constructed inland. Yet, growing evidence suggests that saltmarshes within MR sites have
79 lower biodiversity and abundance of key species than anticipated (e.g. Mazik et al., 2010;
80 Mossman et al., 2012), which may have consequences for ecosystem functioning (Doherty

81 et al., 2011). These differences have been associated with abiotic factors such as nutrient
82 availability, salinity and redox conditions (Erfanzadeh et al., 2010; Mossman et al., 2012).
83 MR is often carried out in areas of former saltmarsh and mudflat habitat, which have been
84 previously reclaimed through the construction of embankments and then drained for
85 agriculture. As a consequence, the practice results in the restoration and re-creation of
86 historical intertidal habitats (as opposed to creating “new” habitats). Reclamation and
87 drainage leads to compaction, de-watering and mineralisation of organic matter, resulting in
88 irreversible changes to the sub-surface sediment structure (including the collapse of pore
89 space) (e.g. Crooks and Pye, 2000; Hazelden and Boorman, 2001; Spencer et al., 2017). This
90 has led to poor drainage in many MR sites following site inundation and reduced vertical
91 hydrological connectivity between the relict terrestrial horizon and the freshly deposited
92 intertidal sediment (e.g. Crooks and Pye, 2000; Hazelden and Boorman, 2001; Tempest et
93 al., 2015).

94

95 The flux of pore water through the sub-surface sediment is considered to be crucial for
96 controlling abiotic conditions, and therefore could exert a major influence on vegetation
97 colonisation in MR sites (Davy et al., 2011; e.g. Howe et al., 2010; Wilson et al., 2015).

98 However, there remains a shortage of data on the evolution of sub-surface sediment
99 geotechnical and geochemical properties following inundation at MR sites (Esteves, 2013).

100 This is especially true for investigations into the critical period immediately following site
101 inundation (i.e. in the early stages of the terrestrial to marine or estuarine transition) as it is
102 these surface conditions that will form the substrate for seedling germination, with
103 particular focus required into:

- 104 (a) the preservation of the relict terrestrial horizon, and its structural, physical and
105 chemical characteristics, post-inundation, and
- 106 (b) the development of the sub-surface geochemical profile in response to the former
107 terrestrial land use.

108

109 This study investigates the impact of different pre-managed realignment land use practices
110 on the early evolution of the sub-surface sediment structure and geochemical environment
111 at the Medmerry Managed Realignment Site (West Sussex, UK), during the first three years
112 of site inundation (covering the early stages of the transition from a terrestrial to a marine /
113 coastal lagoonal system). Specifically, a novel combination of broad- (centimetre to
114 decimetre) and intensive- (micron) scale sedimentary data sets, from samples taken at two
115 time points, are analysed to assess the differences and the early evolution of the sub-
116 surface geochemical profile and sediment structure for sites of differing former land use.
117 The implications of these differences for the longer term development of sediment
118 structure, drainage and physicochemical properties, in relation to site evolution,
119 management, and ecosystem service delivery, are discussed and assessed.

120

121 **3 Study Site**

122

123 The Medmerry Managed Realignment Site (Figure 1) is located within the Solent, southern
124 UK, on the western side of the Manhood Peninsula (Figure 1, insert). Previously, the area

125 had been a brackish lagoon (Krawiec, 2017) behind a shingle barrier beach, which had
126 drained through Pagham Harbour on the eastern side of the peninsula. However, this area
127 was separated from Pagham Harbour and reclaimed through the construction of an
128 embankment, and subsequently drained, between 1805 and 1809 (Bone, 1996). Coastal
129 flood defence for the reclaimed area at Medmerry was provided by the shingle barrier
130 beach, which was managed by the Environment Agency (UK). To maintain the necessary
131 defence standard, constant work was required each winter to recycle and re-profile the
132 shingle bank. Nevertheless, the defences remained vulnerable during storm events; the
133 bank was breached 14 times between 1994 and 2011, flooding homes, local holiday caravan
134 parks and agricultural land. The coastal flooding and erosion risk was reviewed in the
135 Pagham to East Head Coastal Defence Strategy (Environment Agency, 2007), which
136 endorsed MR as the most suitable method of managing the risk of coastal flooding.

137

138 The Medmerry scheme, which is the largest open coast MR site in Europe (at the time of site
139 inundation), was designed not only to provide a sustainable and cost-effective method of
140 coastal flood risk management, but also to compensate for saltmarsh and mudflat habitat
141 loss elsewhere in the region. Over 80% of the Solent's coastline is designated for its nature
142 conservation interest (Foster et al., 2014), yet 40% (approximately 670 hectares) of
143 saltmarsh in the region were lost through erosion between 1971 and 2001 (Cope et al.,
144 2008). Over the one hundred years following construction of the Medmerry site, it was
145 estimated that up to 184 hectares of new intertidal and transitional habitat would be
146 created (Pearce et al., 2011).

147

148 Construction of the site began in autumn 2011, which included 7 km of new earth “bund”
149 defences, reaching 3 km inland. Freshwater drains through the site via four drainage outlets
150 with tidal gates constructed into the new defences. The site was breached on 9th
151 September 2013 through a single narrow opening in the shingle bank, forming a semi-
152 diurnal, mesotidal, semi-enclosed, fetch and depth limited estuarine system. At the time of
153 this study, high water at the furthest point inland occurred approximately 50 minutes after
154 high water at the breach (Dale et al., 2018b). During low tide, draining water is constricted
155 to the main channels running through the site (Figure 1), which in some cases drain to near
156 emptiness. Sediment is imported, and exported, from the wider coastal environment, but
157 Dale et al. (2018b) identified that larger concentrations are currently being internally
158 redistributed as the site responds to the introduction of intertidal inundation.

159

160 **4 Materials and Methods**

161

162 Six sediment cores were taken from the Medmerry site in each of 2015 and 2016. All
163 sampling was performed at low water. Cores 1 to 4 were collected for broad-scale analysis,
164 Cores 5 and 6 for intensive-scale analysis. Sampling was carried out at four locations within
165 the Medmerry site. These locations were selected based on differences in former
166 (terrestrial) land use. Cores 1 and 5 were taken from a former area of pastoral land,
167 occasionally used for low quality (usually unsuccessful) arable agriculture. Cores 2 and 3
168 were from a former area of pastoral land, with Core 2 taken from a non-vegetated surface
169 and Core 3 from a vegetated surface. Cores 4 and 5 were from a former intensive arable
170 field, last harvested two weeks prior to site inundation, behind an area of lower elevation
171 land which has experienced rapid accretion of coarse grained sandy sediment ($d_{50} = 47.33 \pm$
172 $0.91 \mu\text{m}$) following site inundation (Dale et al., 2017). The expected differences in sediment
173 structure as a result of the former land use are outlined in Table 1. The presence and extent
174 of these proposed differences were assessed initially on a broad centimetre scale, followed
175 by analysis carried out on an intensive (micron) scale.

176

177 **4.1 Sampling and Methods for Broad (centimetre to decimetre)-Scale Analysis**

178

179 Vertical sediment cores were taken in January 2015, 16 months after the site was breached,
180 and September 2016, 36 months after site inundation, to evaluate differences in the
181 sediment sub-surface physical properties and geochemistry. Two cores were taken in

182 parallel, at approximately the same elevation (± 2 cm) and within 30 cm of each other, at
183 each sampling location using a hand driven large (5cm diameter, stainless steel) gouge
184 corer, transferred to open PVC tubes and wrapped in PVC film. Due to topographic
185 variations within the site it was not possible to sample at identical elevations at the four
186 sampling sites, but all sites were approximately in the same position in the intertidal zone
187 and therefore are expected to have similar hydroperiod conditions. Core depths varied
188 between 26 and 49 cm, although parallel cores were not always taken to the same depth.
189 Sediment cores were collected at least 15 m from the channel to minimise the influence of
190 lateral sub-surface flow (Marani et al., 2006).

191

192 Samples were stored at + 3.6 °C until analysis. Sediment properties were visually described
193 and one core from each site was subsampled at 1 cm depth increments. Following hydrogen
194 peroxide treatment and dispersion with sodium hexametaphosphate, a Malvern
195 Instruments Mastersizer Hydro 2000G Laser Diffraction Particle Size Analyser was used to
196 determine the grain size distribution in sediment subsamples. Subsamples were also
197 examined for a suite of elements using an Inductively Coupled Plasma-Optical Emission
198 Spectrometer (ICP-OES). Samples were digested with Aqua Regia (modified from Berrow
199 and Stein, 1983). Aqua Regia was prepared with a 30% HNO₃ : 70% HCL (1:3) mixture at
200 room temperature. 0.1 ± 0.01 g of sample, oven dried at 105 °C, was digested in 3 ml of
201 Aqua Regia for three hours in a water bath at 80 °C. Following digestion, 7 ml of distilled
202 water were then added to the sample. A 1:10 dilution of the solution was made with
203 distilled water for analysis using a Perkin Elmer Optima 2100 DV ICP-OES. To assess the
204 elemental recovery of the digestion procedure the measured values were compared to the

205 quoted values for a Certified Reference Material (CRM) digested and analysed alongside the
206 samples (e.g. Cochran et al., 1998). The Mess-4 Marine Sediment (National Research Council
207 Canada) CRM was used and recovery values were generally within $\pm 25\%$ of the reported
208 values (see supporting information). Process blanks and repeat samples were analysed
209 every 20 samples for quality control and analytical error. Process blanks were below
210 detection limits and repeat samples were within $\pm 10\%$ throughout.

211

212 For the remaining cores, a known quantity of sediment was extracted using a syringe at 1
213 cm intervals and analysed for wet bulk density, moisture content, porosity and loss on
214 ignition (a proxy for organic content). The moisture content was measured as a percentage
215 of the dry mass (moisture content = water weight / dry sediment weight x 100) after
216 samples had been oven dried at 105 °C for 48 hours. Porosity was calculated using the dry
217 bulk density, assuming a particle density of 2.65 g cm⁻³ as stated by (Rowell, 1994) based on
218 typical data. The organic content of the samples was estimated via the loss on ignition proxy
219 method, following ignition of subsamples for six hours at 450 °C.

220

221 **4.2 Sampling and Methods for Intensive (micron)-Scale Analysis**

222

223 Smaller sediment cores were recovered from the same coring locations as Core 1 and Core
224 4, labelled Cores 5 and 6 respectively, in July 2015 and September 2016. These sites were
225 selected to analyse the influence that different intensities of arable agricultural activity have
226 on the subsurface sediment structure (i.e. by using sites with / without a history of intensive

227 arable agriculture). Cores were taken from within 2 m of the broad-scale coring sites, using
228 the advanced trimming method (Hvorslev, 1949). 44 mm diameter clear PVC tubes were
229 inserted into the sediment, trimming the surrounding sediment to minimise the disturbance
230 to the sample. Core lengths varied between 7.9 cm and 11.1 cm. The ends of the sample
231 tubes were capped and wrapped in PVC film secured with tape to prevent moisture loss.
232 Cores were kept upright during transport and storage to minimise any disturbance and, on
233 return to the laboratory, were stored between + 3.6 °C and + 4 °C.

234

235 3D-computed X-ray microtomography (μ CT) is a non-destructive imaging method that has
236 been successfully applied to the study of saltmarsh sediment structure (Cnudde and Boone,
237 2013; Ketcham and Carlson, 2001; Spencer et al., 2017). μ CT analysis was carried out here to
238 identify the sediment bulk phases and stratigraphy (for an assessment of the comparability
239 of the broad- and intensive-scale methodologies) and to analyse the key structural and
240 stratigraphic differences (total porosity, characterisation of the pore networks) between the
241 two sampled sites, at a much higher resolution than the broad-scale approach described
242 above. Whilst only single core samples were analysed in both years per core site, previous
243 analysis of this type (e.g. Spencer et al., 2017) has recognised that single core samples may
244 be used as a representation of the sediment structural characteristics. Sealed core tubes
245 were scanned at 76 μ m resolution using a Nikon Metrology XT H 225 X-ray CT system with
246 Perkin Elmer XRD 0820 CN3 16-bit flat panel detector at Queen Mary, University of London.
247 Inspect-X was used to perform the scans and X-radiogram acquisition and reconstruction
248 was undertaken in CTPro. Drishti 2.1 volume rendering software was used for visualisation
249 of the reconstructed 3D models to identify bulk phases and inform segmentation following

250 the method of Spencer et al. (2017). Each 3D volume was sub-sampled further into four
251 equally sized depth increments, labelled A (base) to D (top), for detailed quantification of
252 differences in porosity with depth.

253

254 Cores were split vertically, photographed and analysed using Itrax non-destructive micro-X-
255 ray fluorescence spectrometry analysis (Croudace et al., 2006) for a range of elemental data
256 to compare changes in geochemistry with sediment structure analysis provided by the μ CT,
257 at a 200 micrometre scale which was not possible using ICP-OES analysis. The Itrax produces
258 elemental data in counts but previous studies (e.g. Miller et al., 2014) have shown that
259 these data correlate well with quantitative analytical data (e.g., ICP-OES or Wavelength
260 Dispersive X-ray Fluorescence). Furthermore, the high frequency compositional changes
261 identified using the Itrax are often missed when analysing lower resolution bulk sub-
262 samples using more traditional, destructive, analytical methods. Each core was loaded onto
263 a horizontal cradle and scanned at a resolution of 200 μ m at the BOSCORF laboratories,
264 National Oceanography Centre (Southampton). Cores were scanned wet to preserve
265 internal structure, with the software correcting for water content. Core Scanner Navigator
266 software was used to control the scanner, and data were plotted and displayed using Q-
267 Spec software. The Itrax scanner combines an X-ray line camera with a narrow, parallel,
268 high-flux X-ray beam to record a radiograph at 55 kV. XRF analysis was performed at 30 kV
269 (using a Mo anode X-ray tube, counting time 30s). Data were plotted using ItraX-Plot,
270 described by Croudace et al. (2006).

271

272 **5 Results**

273

274 **5.1 Broad-scale (centimetre to decimetre) Physicochemical Changes in the** 275 **Subsurface (Cores 1 to 4, 2015 and 2016)**

276

277 Sediment cores 1 to 4 exhibited clear vertical zonation and could be divided into three facies
278 (from core base to core surface) based on the environmental and land use change known to
279 have occurred at the Medmerry site; (i) a pre-reclamation intertidal unit (*Unit A*), (ii) a
280 reclamation boundary and soil unit formed since site reclamation between 1810 and 1880
281 (*Unit B*), and (iii) a terrestrial boundary and post-breach intertidal unit dating from site
282 inundation in September 2013 (*Unit C*). The depth, composition and structure of the three
283 units varied between sites.

284

285 **5.1.1 Physical Characteristics**

286

287 Average physical sediment characteristics for the three units are presented in Table 2 (see
288 supplementary material for core descriptions and full datasets). Wet bulk density ranged
289 from 0.64 to 2.18 kg m⁻³ and tended to increase with depth. Both moisture content (36.62 –
290 123.08 %) and porosity (0.33 – 0.81) decreased with depth, whereas loss on ignition values
291 varied from 3.24% to 19.21% and fluctuated through the sample. Coarser grained sediments
292 were generally found in the Unit A, compared to Units B and C, except in Core 4 where
293 coarser grained sediments ($d_{50} = 67.87$ (2015) and 49.77 (2016)) were found at the sediment

294 surface. Median grain sizes ranged from 5.46 to 46.48 μm , and the mud content (clay + silt)
295 varied between 54.1 and 97.67 %. Statistical differences between sediment units were
296 assessed via a Kruskal Wallis test ($n = 22$ to 45 , $p < 0.05$) for the whole dataset with the
297 exception of Core 4₁₆ as no vertical zonation was found in this sample. Statistical differences
298 were found between the three sediment units for all parameters except for particle size
299 analysis (median grain size and mud content).

300

301 **5.1.2 Geochemical Profiles**

302

303 ICP-OES-derived major element data (Al, Ca, Fe, Mn, S, Na) are presented for 2015 (Figure 2)
304 and 2016 samples (Figure 3). To account for variations in sediment composition, data have
305 been normalised to Al (after Spencer et al., 2008). Ca decreased with depth through Unit C
306 in all 2015 samples and Cores 2 and 3 in 2016. This may be the result of decalcification,
307 typical of oxic saltmarsh sediments as a result of a lowering of the pH caused by nitrification
308 and decomposition of organic matter (Luther and Church, 1988; Vranken et al., 1990), and
309 then re-precipitation at depth. However, the scale of the decrease, and subsequent increase
310 in Unit A (Core 1₁₅ and Core 4₁₅) could also be indicative of the presence of finely
311 comminuted shell debris in the intertidal sediments (Units A and C).

312

313 The diagenetic cycles of Fe and Mn have been well documented for saltmarsh sediments
314 (e.g. Spencer et al., 2003; Zwolsman et al., 1993). A peak in Fe or Mn concentration may
315 indicate redox mobilisation and reprecipitation, whereas an increase in S may represent

316 bacterially-mediated reduction of sulphate and formation of early-diagenetic sulphide
317 minerals (Cundy and Croudace, 1995). In both years at coring locations 1, 2 and 4, and in
318 Core 3₁₅, Fe and Mn concentrations were relatively homogenous down core with some
319 variability within Unit B, potentially caused by residual Fe concretions from the legacy of
320 ploughing within this zone, without any consistent or clear peaks. This is suggestive of a
321 fluctuating water table through the sediment sub-surface, consistent with the visual
322 observations of Fe-stained mottled sediment in this zone (see supplementary material); this
323 may be the result of tidal variability causing changes in the redox boundary, preventing the
324 formation of a stable redox zone and a strong Fe and Mn peak (Cundy and Croudace, 1995;
325 Zwolsman et al., 1993). However, in Core 3₁₆, Fe fluctuated throughout the depths
326 examined, peaking in the middle terrestrial zone. A clearer trend was observed in the
327 concentration of Mn, which is more sensitive than Fe to changes in redox status, with Mn
328 peaking at the boundary between the post-breach intertidal and terrestrial facies suggesting
329 possible diagenetic enrichment of Mn. S concentration decreased with depth, matching the
330 changes in Na concentration, and therefore implying that variations in S are driven primarily
331 by the introduction and evaporation of sea water.

332

333 Principal component analysis (PCA) was performed on the entire dataset to differentiate
334 between the physical and geochemical characteristics of the different units. PCA is a data
335 reduction technique which calculates new variables, or principal components, from linear
336 combinations of the original parameters and has been used successfully elsewhere to
337 (partially) discriminate geochemical data in coastal sediments (e.g. Cundy et al., 2006). The
338 first principal component accounts for the greatest variability, with every subsequent

339 component accounting for less of the variability (Reid and Spencer, 2009). Therefore, PCA
340 allows for grouping of different depths based on their physicochemical variability. Results
341 reveal clear differences between the PCA scores for Units A and C (Figure 4). Unit B also
342 demonstrated some evidence of grouping, but overlapped the other two units.

343

344 **5.2 Intensive-scale (micron) Subsurface Structure Physicochemical Characteristics**

345

346 **5.2.1 Sediment Structure**

347

348 Representative μ CT reconstructions of sediment structure, with a voxel size of 65 μ m, are
349 presented for coring locations 5 (taken from an area of former lower intensity arable
350 agriculture) and 6 (an area of former high intensity arable agriculture) in Figure 5. Core 5
351 demonstrated a relatively consistent solid matrix phase (Figure 5a) in both years sampled,
352 with no separate sediment facies, suggesting there has been no (or very minimal) post-site
353 inundation deposition of sediment. This is despite the broad-scale geophysical analysis
354 suggesting that a small, 2 cm, new intertidal sediment unit was present. It is, therefore,
355 possible that these different units might be present, but that they are sufficiently similar in
356 sediment structure to be indistinguishable via μ CT analysis. In contrast, structural
357 differences were clearly visible in Core 6₁₅ (Figure 5b). Laminations were present in a
358 compact upper sediment facies, consisting of sandy sediment deposited following site
359 inundation, overlying the former terrestrial soil that had been used intensively for arable
360 agriculture up to two weeks prior to site inundation. A sharp, irregular boundary occurred
361 between the two units and is marked on Figure 5b. No evidence of the upper sediment

362 facies was found in the Core 6₁₆ sample (Figure 5b), probably due to the local remobilisation
363 of sediment in response to observed changes in the site's hydrodynamics, and
364 morphological evolution in response to the introduction to intertidal inundation (Dale et al.,
365 2018a).

366

367 Macroporosity (pores > 80 µm; Beven and Germann, 2013) measurements and
368 characteristics are presented in Table 3, and plotted for each of the four sub-samples in
369 Figure 6. In Core 5₁₅, a large, interconnected, pore space was detected through the sample,
370 whereas the Core 5₁₆ pore structure consisted of horizontal elongated macropore networks.
371 In Core 6₁₅, a sheet like macro-pore was detected across the division between the units,
372 although it is likely that this an artificial feature caused by the coring process (which
373 resulted in sediment cracking along this interface), with a large horizontal macropore
374 dominating the lower facies. There was also no evidence of this horizontal pore system in
375 Core 6₁₆, with the macropore network dominated by a vertical pore (on the left of the 2016
376 macro-pore phase in Figure 5b) and areas of isolated, flattened pore space.

377

378 Bulk macroporosity in Core 5 was generally moderate to high (5.6 – 22.4 %) and decreased
379 with depth (Figure 6), as would be expected due to sediment compaction effects. Less
380 variability was observed in Core 6, where bulk macroposity was low to moderate (3.5 – 13.1
381 %). The degree of pore connectivity is indicated by the Euler-Poincaré characteristic, a
382 measure of the number of redundant connections within the pore network expressed as a
383 function of the volume, with decreased connectivity indicated by increased positive values,

384 and increased connectivity demonstrated by decreased negative values (Vogel, 1997). All
385 samples followed a trend of decreasing connectivity upwards, and then increasing in the
386 upper sub-sample, reflecting an increase in redundant connections and more tortuous pore
387 networks in the upper and lower sediment sub-sections. Connectivity was greater in 2015
388 compared to 2016 at both sites and was greater in Core 5 compared to Core 6, suggesting
389 greater levels of compaction due to higher levels of agricultural activity and an increase in
390 compaction at both sites as each evolved following site inundation.

391

392 The mean number of branches per pore were calculated through the transformation of
393 macropores into topological networks of nodes and branches, and used as an indication of
394 pore network complexity (Polder et al., 2010). Pore networks were more complex in Core 6
395 than Core 5, but at both sites decreased in complexity between 2015 and 2016. This
396 suggests that pore system complexity decreases over time following site inundation, due to
397 either the hydraulic head of tidal water above the sediment causing compaction or
398 sediment being flushed out as the water drains causing the pore networks to collapse (Dale
399 et al., 2018a). No distinct pattern was present in the Core 5₁₅, but in Core 5₁₆ the upper sub-
400 sample had a greater number of branches per pore compared to the rest of the sample. In
401 contrast, complexity in Core 6 decreased upwards, but increased in the upper sub-section
402 consisting of the post-breach sediment facies. The degree of anisotropy is representative of
403 similarity in arrangement and the directness of the branches of the dominant macropore
404 system (Odgaard, 1997). In 2015, pores were more aligned in Core 5 than Core 6, although
405 anisotropy was much lower in the basal sub-samples of Core 5 (A and B). Anisotropy was
406 higher in the post-breach sediment facies in Core 6₁₅. In comparison, macropores

407 demonstrated a similar level of organisation in Core 5₁₆, whereas Core 6₁₆ had a higher
408 anisotropy value representing an increase in similarity in the arrangement of the pore
409 networks.

410

411 **5.2.2 Sediment Geochemistry**

412

413 Itrax scanning was employed to examine the variability of nine elements at high spatial
414 resolution (200 µm). The content of coarse grained sediment, indicated by the Zr and Cr
415 intensity (which are frequently associated with heavy mineral assemblages in detrital sands,
416 e.g. Cundy et al., 2006), remained relatively constant in Core 5₁₅ (Figure 7a). Two major
417 peaks were observed in the Cr intensity, although the second of these peaks corresponded
418 with an area of high intensity present on the radiograph likely to be a clast. Measurements
419 of the K intensity indicate that the fine grained fraction decreased in the middle section of
420 the sample, increasing again deeper in the sample, which is also reflected in Si and the bulk
421 µCT attenuation measurements (Figure 5a). Similar trends were observed in the Cl and Ca
422 intensity. Black sediment, low Fe and Mn, and a peak in S, suggest possible bacterial
423 reduction of sulphate within the cracked and desiccated near-surface sediments (Figure 5a),
424 although broadly coincident peaks in Cl and Ca may indicate that the peak in S is at least
425 partly a function of increased porewater sulphate rather than sulphate reduction processes.
426 Fe and Mn increased below this unit and remained constant throughout the rest of the
427 sample, with three relatively large peaks. However, the Fe peaks corresponded with peaks
428 in X-ray intensity (kcps) and are likely to be the product of X-ray response rather than

429 increases in concentration. After peaking in the near-surface sediment, S followed a similar
430 pattern to Si, K, Cl and Ca.

431

432 No major vertical changes in bulk sediment composition were detected in Core 5₁₆ (Figure
433 7b), demonstrated by the relatively constant distribution of Si with the major peaks
434 corresponding to variability in the X-ray response (kcps). These observations were
435 supported by similar trends in Zr and Cr intensities, although peaks were also observed in
436 these elements corresponding to the presence of high density material (clasts, evident in
437 the X-radiograph image). The distribution of K indicated relatively constant clay content
438 within the sample. Cl decreased slightly down-sample, whereas Ca decreased in the lower
439 section of the sample, indicative of decalcification. In contrast to the other elements, Mn
440 showed a strong increase in intensity in the middle part of the core, possibly reflecting early
441 diagenetic enrichment, although this observation was not supported by change in the Fe
442 intensity. However, analysis of the Fe / Mn ratio (Figure 8) indicated higher concentrations
443 of Mn to Fe in the middle of the core, suggesting mildly reducing conditions and early
444 diagenetic mobilisation of Mn. No evidence of the bacterial reduction of sulphate, possibly
445 present in the near-surface of the previous sample, was found, and trends in S generally
446 coincided with peaks in Cl and Ca so may be caused by increased porewater sulphate rather
447 than microbially-mediated sulphate reduction.

448

449 Coarse grained sediments dominated the near-surface component of Core 6₁₆ (Figure 7c),
450 visible in the photographic image and indicated by the high intensity of Zr. Several peaks in

451 Cr were detected in the upper part of the core, likely to correspond to the laminations
452 observed in the μ CT scan (Figure 5b). At the boundary between the post-breach and
453 terrestrial sediment facies Cr peaked below a unit of low density detected by the
454 radiograph, matching the sheet-like pore space present in the μ CT scan (Figure 5b). Below
455 this unconformity, K intensity increased, and Zr / Cr decreased, indicating an increase in fine
456 grained sediment. Cl generally decreased through the sample, whereas Ca decreased and
457 then increased again. Evidence of sub-surface diagenetic enrichment of Mn was provided by
458 an increase, and peak, in intensity in the lower third of the core. The peak in Mn
459 corresponded to an area of low density measured by the radiograph, although this is not
460 visible on the photography. It is possible that this area is the large horizontal macro-pore
461 feature present in the μ CT analysis. The concentration of Fe also increased through the
462 sample, with areas of enrichment corresponding to red mottling on the sample. The Fe / Mn
463 ratio decreased through the upper 2 cm of the sample (Figure 8), but increased again at a
464 similar depth to the large horizontal macro-pore. Below the terrestrial boundary, S intensity
465 decreased through the sample. Small scale increases in S intensity occurred in areas where
466 red mottling of the sediment was not present.

467

468 In Core 6₁₆ (Figure 7d) coarser grained sediments were only found in the surface sediment,
469 indicated by the surface peak in Zr, consistent with the findings from the broad-scale and
470 μ CT analysis. Trends in K suggested increased clay content was present in the middle of the
471 sample. A peak in Cl occurred within the upper sub-surface, corresponding to a peak in S,
472 which could indicate the depth of saline intrusion into the sediment. Fe and Mn decreased
473 through the top of the red mottled surface sediment. Fe, and to a lesser extent Mn,

474 increased through the middle of the sample, supporting visual observations of red mottling,

475 with an additional increase present in the deeper parts of the sample.

476

477 **6 Discussion**

478

479 **6.1 Preservation of the Pre-Breach Terrestrial Surface**

480

481 Observations made at other, older, MR sites suggest that visual changes in the sediment
482 characteristics associated with a terrestrial boundary or horizon would no longer be present
483 after a number of years. For example, no visual evidence of a terrestrial facies was found at
484 Orplands Farm Managed Realignment Site 8 years after site inundation (Spencer et al.,
485 2008), although at this site a terrestrial horizon could still be detected through analysis of
486 physicochemical properties of the sediment. Broad-scale analysis from four locations at the
487 Medmerry Managed Realignment Site provided visual evidence that a sub-surface
488 unconformity could still be detected at all sites except for Core 4₁₆, the nearest site to the
489 breach (in a significantly higher energy environment than the other sites sampled).

490 However, no uniform stratigraphic marker of the terrestrial surface such as the organic rich
491 peaty horizon identified at Pagham Harbour by Cundy et al. (2002) or the alternating peat-
492 mud (i.e. terrestrial – marine) couplets used elsewhere as indicators of tectonic activity and
493 sea level change in coastal and near-coastal sediments (e.g. Shennan et al., 1996; Shennan
494 et al., 1998) was found, although these have been suggested to be inconsistently preserved
495 in some suddenly submerged intertidal environments (Cundy et al., 2000). In each sample
496 where a sub-surface unconformity was detected, a lower pre-reclamation sediment facies
497 was also detected. PCA allowed (partial) discrimination of samples based on combined
498 physical and geochemical sediment properties, as opposed to a single indicator such as loss

499 on ignition or changes in particle size, into groups which corresponded to one of the three
500 vertical sediment facies; post-breach, terrestrial or pre-reclamation sediments.

501

502 The reclamation of saltmarshes results in modification to sediment structure and properties
503 (e.g. Crooks et al., 2002; Hazelden and Boorman, 2001) as a result of de-watering and
504 organic matter mineralisation, decreasing the porosity and increasing the bulk density. After
505 the re-introduction of intertidal conditions through MR, the legacy of these changes can still
506 be detected, with low moisture contents still being found at depth several decades after site
507 inundation (Spencer et al., 2017). Analysis of sites of different former land use at Medmerry,
508 16 months after site inundation, indicated similar bulk densities and porosities within the
509 terrestrial facies regardless of former site activity and land use. However, moisture content
510 and loss on ignition were higher in Cores 2 and 3, areas which previously had not been
511 subjected to arable agricultural practices (i.e. ploughing).

512

513 Detailed examination of the 3D sediment structure through the use of μ CT allowed
514 comparisons of the morphology and connectivity of the sediment macro-porosity at
515 different coring locations to be made. In Core 5, taken from a site that was previously used
516 occasionally (and usually unsuccessfully) for agriculture, no new intertidal sediment unit was
517 detected despite evidence of separate units in the broad-scale analysis. It is possible that
518 differences observed in the broad-scale analysis are the result of the terrestrial unit
519 transitioning into an intertidal sedimentary environment, rather than consisting of sediment
520 deposited following site inundation. This is reflected in the similarity in the matrix of the

521 sediment detected by the μ CT analysis and the gradual transition between the units
522 observed in Core 1₁₆. Core 5 had a greater bulk macroporosity throughout the sediment
523 sub-surface, with simpler pore networks that were more connected and had greater
524 similarity in arrangement than Core 6, which had been used consistently for high intensity
525 agricultural activity. This indicates that, as a result of the legacy of different terrestrial
526 agriculture practices, different sub-surface structures exist in terms of sediment
527 macroporosity, which is likely to affect the drainage characteristics and therefore
528 geochemical profiles within the sediment subsurface. Terrestrial and post-breach facies
529 were detected in the 2015 3D sediment structural analysis performed on Core 6. The top
530 facies consisted of laminated sediment deposits, which had accreted post-site inundation.
531 When re-sampled, only one sediment facies was detected. This is potentially the result of
532 local remobilisation of intertidal sediment deposited post-site inundation, likely to be in
533 response to changes in site hydrodynamics and morphological evolution as the realignment
534 site evolves.

535

536 Analysis of physical characteristics and structure of the sediment at Medmerry indicate
537 differences in sediment composition, properties and macroporosity for sites of differing
538 former land use, with the terrestrial soil unit still detectable visibly at some sites up to three
539 years after site inundation. These differences may well have consequences for the
540 development of geochemical profiles, which might limit the colonisation of saltmarsh
541 vegetation (Davy et al., 2011) and explain the lower biodiversity and abundance of key
542 species observed elsewhere (e.g. Mazik et al., 2010; Mossman et al., 2012). Importantly,
543 however, levels of sediment accretion over the terrestrial unit were much lower than at

544 other older sites (typically 20 to 40 mm at Medmerry compared to, for example, *ca.* 60 mm
545 at Orplands Farm) (Spencer et al., 2008), which may partly mitigate any discontinuities in
546 hydrological connectivity caused by the deposition of intertidal sediment on top of the
547 preserved terrestrial surface.

548

549 **6.2 Implications for Geochemical Profile Development at Managed Realignment** 550 **sites**

551

552 Typical vertical saltmarsh geochemical profiles are controlled by strong physicochemical
553 gradients in pH and redox potential, and microbially-mediated organic matter breakdown
554 using electron acceptors such as O₂, MnO₂ and Fe(OH)₃ (e.g. Koretsky et al., 2005; Spencer
555 et al., 2003). Following reclamation and ploughing large-scale precipitation of Fe
556 oxyhydroxides and other Fe-rich minerals would be anticipated (Auxtero et al., 1991;
557 Violante et al., 2003). When re-introduced to intertidal conditions remobilisation of Fe by
558 the saline water is expected through dissimilatory reduction of sulphate or dissolved Fe
559 being re-distributed by advection caused by the local hydrology (Burton et al., 2011;
560 Johnston et al., 2011). However, impeded vertical solute and porewater transport caused by
561 the presence of an aquaclude-like boundary in the sediment sub-surface (e.g. Tempest et
562 al., 2015) may result in inadequate drainage, stagnant porewater and a lack of aeration. The
563 occurrence of these conditions will inevitably prevent the formation of suitable oxic
564 conditions for re-precipitation of Fe, and Mn, at the sediment surface (Spencer et al., 2008).

565

566 No evidence of an aquaclude was found in either of Cores 2 and 3. In Core 2₁₅, Fe peaked at
567 the terrestrial boundary, corresponding to a peak in loss on ignition values. The increase in
568 residual bulk organic matter, present on the terrestrial surface before site inundation, may
569 well drive bacterially-mediated sulphate reduction following incorporation into the
570 sediment, resulting in the enrichment of Fe via Fe-sulphide formation. No major trends
571 were detected in Fe content through the rest of the sample, where the sediment showed
572 clear red mottling, implying variability in the water table caused by tidal inundation (Cundy
573 and Croudace, 1995). Fe fluctuated through the red mottled Core 3₁₅, indicating a
574 fluctuating water column through the sub-surface sediment.

575

576 Core 2₁₆ was visibly darker in the intertidal and terrestrial facies, decreasing in S and
577 increasing in Fe and Mn to the boundary between the units. The sharp nature of this
578 boundary, and the peak in moisture content may indicate reduced vertical conveyance of
579 water through the unconformity. The fluctuations in Fe, and to a lesser extent Mn, in the
580 pre-reclamation intertidal facies could be caused by trapping authigenic carbonate /
581 sulphide formation (Cundy and Croudace, 1995). In Core 3₁₆, the distribution of Fe
582 continued to indicate a fluctuating water column.

583

584 Broad- and intensive-scale analysis suggests evidence of bacterial reduction of sulphate at
585 the surface of Core 1₁₅ and Core 5₁₅. Below this unit the red mottled sediment and Fe profile
586 implied a variable water column facilitated by the extensive inter-connected macro-pore
587 network indicated by μ CT analysis. An increase in the Fe / Mn ratio in the middle of the

588 sample analysed using high resolution Itrax scanning in Core 5₁₆ suggests redox mobilisation
589 of Mn, which is generally more sensitive to redox changes than Fe. Despite the differences
590 in sediment structure between Core 5 and 6, there was still evidence of Fe enrichment. The
591 macro-pore network was dominated by a large horizontal pore which corresponded to an
592 increase in the intensity of Mn and the Fe / Mn ratio in Itrax data, possibly the result of
593 enrichment via lateral through-flow and indicative that the pore was not an artificial by-
594 product of the sampling procedure. These trends were maintained when re-sampled with
595 no sub-surface unconformity detected in Core 6₁₆. Results presented here differ from the
596 geochemical and redox profiles observed in older MR sites (Spencer et al., 2008), and
597 natural saltmarsh and mudflat environments within the Solent (e.g. Cundy and Croudace,
598 1995). It remains to be seen if the geochemical profiles evolve in a similar manner to other
599 MR sites or towards that of a more typical intertidal setting, compared schematically in the
600 Graphical Abstract, and the timescales required for this development. Not only would this
601 determine the depth of any anoxic layer, which may inhibit biological activity, but will
602 influence nutrient exchange and the partitioning (and possibly release) of contaminants
603 such as metals or pesticides potentially stored within the sediment.

604

605 **6.3 Influence of the Former Land Use and Site Construction**

606

607 MR aims to restore the structure and functioning of intertidal habitats, compensating for
608 losses elsewhere. However, previous studies have demonstrated differences in the physical,
609 geochemical and hydrological characteristics of saltmarshes in MR sites, particularly at the
610 Orplands Farm site (UK), compared to natural marshes (Spencer et al., 2017; Spencer et al.,

611 2008; Tempest et al., 2015). This has resulted in the restoration of intertidal conditions, but
612 not full restoration of the hydrological regime and the physical structure of the intertidal
613 environment which may have consequences for the ecological functioning and ecosystem
614 services provided. It has been proposed that the structural differences between MR and
615 natural sites are the cause of water-logging and poor drainage, which have been attributed
616 to poor saltmarsh species abundance and diversity within MR sites (e.g. Mossman et al.,
617 2012). Clear differences in sediment structure for sites of different former land use were
618 found at the Medmerry Managed Realignment Site. Therefore, it would be anticipated that
619 sites with reduced porosity and pore connectivity would have lower subsurface flow, no or
620 low concentrations of dissolved oxygen, and anoxic sediment. However, analyses of the
621 geochemical profiles at Medmerry do not yet match this expectation.

622

623 Medmerry is still a developing site on the open coast and, therefore, has not experienced a
624 large accretion of intertidal sediment on the former terrestrial land surface, such as
625 observed in older MR sites found in sediment-rich estuarine environments (Spencer et al.,
626 2017; Spencer et al., 2008; Watts et al., 2003; Wolanski and Elliott, 2016). It remains to be
627 seen how the geochemical profiles develop following further accretion of sediment.

628 However, without the accretion of sediment on top of the terrestrial horizon, tidal waters
629 appear to have been able to drain through the terrestrial facies. An exception is the site of
630 Core 2; in the second sample taken from this site sediment appeared black and anoxic, with
631 evidence of water pooling at the terrestrial boundary and reduced hydrological connectivity
632 through the contact between the facies. These findings suggest that hydrological and
633 geochemical differences found in MR sites compared to natural saltmarshes are not caused

634 by sub-surface differences owing to the former land use, but by the formation of an
635 unconformity in the sediment column as a result of (a) the accretion of sediment, and (b)
636 sharp physicochemical contrasts between the accreted upper unit and the underlying
637 sediment. For the latter, in Core 2, it is likely that the formation of an anoxic unit has been
638 driven by the decay of terrestrial vegetation trapped and buried under the accreted
639 sediment following site inundation (French, 2006).

640

641 **7 Conclusion**

642

643 In this paper, differences in the sub-surface structure and physiochemical properties of
644 inundated sites with different former land use histories have been investigated at the
645 Medmerry Managed Realignment Site, during the initial 16 and 36 months after site
646 inundation. A novel combination of repeated broad- and intensive-scale analysis was used
647 to assess differences in the subsurface sediment structure and early geochemical evolution
648 in the three years following site inundation. Results indicate a number of new findings,
649 including:

- 650 • Clear differences are present in the sediment structure and properties at different
651 sites as a result of contrasts in the former land use. Broad-scale analysis suggests
652 sites formerly used more intensively for agricultural purposes have lower moisture
653 content and loss on ignition, with intensive-scale analysis suggesting pore networks
654 were more complex but were less connected and aligned at these sites.

655 • Evidence of reduced drainage and anoxic conditions, identified in previous studies
656 (e.g. Spencer et al., 2017; Tempest et al., 2015) as a result of modifications caused by
657 a site's terrestrial history, were not found at Medmerry except at the site which had
658 experienced the highest level of accretion (*ca.* 7 cm in 36 months).

659

660 Further work is now required to assess if the differences in sediment structure, identified in
661 this study, can be detected in other (including older) MR sites where greater levels of post-
662 site inundation accumulation have occurred. The findings in this study indicate that the
663 formation of an aquaclude, reducing vertical solute transfer between facies, is not a direct
664 consequence of changes to the sediment caused by the former land use, but is the result of
665 the accretion of sediment, coupled with sharp physicochemical contrasts between the
666 accreted upper layer and the underlying sediment. Many MR sites are designed to
667 accumulate sediment, but these findings highlight the need for improved awareness of
668 sediment accretion in decision-making in the design of MR sites, alongside hydrodynamic
669 and topographic considerations. While further work on other MR sites is needed to assess
670 how widespread this accretionary effect is, the data presented here indicate that sites need
671 to be designed to encourage rapid accumulation of intertidal sediment, burying the
672 terrestrial boundary and so minimising the effect of an aquaclude. Alternatively, predictions
673 need to be adjusted to anticipate reduced saltmarsh diversity abundance, and therefore
674 ecosystem services delivery, until sufficient sediment has been accreted.

675

676

677 **Acknowledgements**

678

679 The authors would like to thank the two anonymous reviewers for their comments, which
680 have helped improve the manuscript. The authors would also like to thank: Matthew Leake
681 (University of Brighton) for his assistance during field work, Magda Grove, Peter Lyons (both
682 University of Brighton) and Lucy Diggins (Queen Mary University of London) for their
683 assistance with laboratory analysis, Callum Firth for his support and guidance during JD's
684 studentship and during fieldwork. X-ray microtomography was carried out by the School of
685 Geography, Queen Mary University of London. The authors are grateful to the BOSCORF
686 facility at the National Oceanography Centre (Southampton) for access to Itrax facilities.
687 Research was funded by the Environment Agency (United Kingdom).

688

689

690 **References**

- 691 Auxtero E, Shamshuddin J, Paramanathan S. Mineralogy, morphology and classification of
692 acid sulfate soils in Pulau Lumut, Selangor. *Pertanika* 1991; 14: 43-51.
- 693 Bergen SD, Bolton SM, L. Fridley J. Design principles for ecological engineering. *Ecological*
694 *Engineering* 2001; 18: 201-210.
- 695 Berrow ML, Stein WM. Extraction of metals from soils and sewage sludges by refluxing with
696 aqua regia. *Analyst* 1983; 108: 277-285.
- 697 Beven K, Germann P. Macropores and water flow in soils revisited. *Water Resources*
698 *Research* 2013; 49: 3071-3092.
- 699 Bone AE. The shaping of the Selsey coastline: a review of the geomorphology, archaeology
700 and history. *Tertiary Research* 1996; 16: 5-14.
- 701 Burton ED, Bush RT, Johnston SG, Sullivan LA, Keene AF. Sulfur biogeochemical cycling and
702 novel Fe-S mineralization pathways in a tidally re-flooded wetland. *Geochimica Et*
703 *Cosmochimica Acta* 2011; 75: 3434-3451.
- 704 Cnudde V, Boone MN. High-resolution X-ray computed tomography in geosciences: A review
705 of the current technology and applications. *Earth-Science Reviews* 2013; 123: 1-17.
- 706 Cochran JK, Hirschberg DJ, Wang J, Dere C. Atmospheric deposition of metals to coastal
707 waters (Long Island Sound, New York USA): Evidence from saltmarsh deposits.
708 *Estuarine Coastal and Shelf Science* 1998; 46: 503-522.
- 709 Cope S, Bradbury A, Gorczynska M. Solent Dynamic Coast Project: Main Report; A tool for
710 SMP2, New Forest District Council/Channel Coastal Observatory, 2008.
- 711 Costanza R, d'Arge R, deGroot R, Farber S, Grasso M, Hannon B, et al. The value of the
712 world's ecosystem services and natural capital. *Nature* 1997; 387: 253-260.
- 713 Crooks S, Pye K. Sedimentological controls on the erosion and morphology of saltmarshes:
714 implications for flood defence and habitat recreation. In: Pye K, Allen JRL, editors.
715 *Coastal and Estuarine Environments: Sedimentology, Geomorphology and*
716 *Geoarchaeology*. 175, 2000, pp. 207-222.
- 717 Crooks S, Schutten J, Sheern GD, Pye K, Davy AJ. Drainage and elevation as factors in the
718 restoration of salt marsh in Britain. *Restoration Ecology* 2002; 10: 591-602.
- 719 Croudace IW, Rindby A, Rothwell RG. ITRAX: description and evaluation of a new multi-
720 function X-ray core scanner. Geological Society, London, Special Publications 2006;
721 267: 51-63.
- 722 Cundy AB, Croudace IW. Sedimentary and geochemical variations in a salt-marsh mud flat
723 environment from the mesotidal Hamble estuary, southern England. *Marine*
724 *Chemistry* 1995; 51: 115-132.
- 725 Cundy AB, Kortekaas S, Dewez T, Stewart IS, Collins PEF, Croudace IW, et al. Coastal
726 wetlands as recorders of earthquake subsidence in the Aegean: a case study of the
727 1894 Gulf of Atalanti earthquakes, central Greece. *Marine Geology* 2000; 170: 3-26.
- 728 Cundy AB, Long AJ, Hill CT, Spencer C, Croudace IW. Sedimentary response of Pagham
729 Harbour, southern England to barrier breaching in AD 1910. *Geomorphology* 2002;
730 46: 163-176.
- 731 Cundy AB, Sprague D, Hopkinson L, Maroukian H, Gaki-Papanastassiou K, Papanastassiou D,
732 et al. Geochemical and stratigraphic indicators of late Holocene coastal evolution in
733 the Gythio area, southern Peloponnese, Greece. *Marine Geology* 2006; 230: 161-
734 177.

735 Dale J, Burgess HM, Burnside NG, Kilkie P, Nash DJ, Cundy AB. The evolution of embryonic
736 creek systems in a recently inundated large open coast managed realignment site.
737 *Anthropocene Coasts* 2018a; 1: 16-33.

738 Dale J, Burgess HM, Cundy AB. Sedimentation rhythms and hydrodynamics in two
739 engineered environments in an open coast managed realignment site. *Marine*
740 *Geology* 2017; 383: 120-131.

741 Dale J, Burgess HM, Nash DJ, Cundy AB. Hydrodynamics and sedimentary processes in the
742 main drainage channel of a large open coast managed realignment site. *Estuarine,*
743 *Coastal and Shelf Science* 2018b.

744 Davy AJ, Brown MJH, Mossman HL, Grant A. Colonization of a newly developing salt marsh:
745 disentangling independent effects of elevation and redox potential on halophytes.
746 *Journal of Ecology* 2011; 99: 1350-1357.

747 Doherty JM, Callaway JC, Zedler JB. Diversity-function relationships changed in a long-term
748 restoration experiment. *Ecological Applications* 2011; 21: 2143-2155.

749 Doody JP. 'Coastal squeeze' - an historical perspective. *Journal of Coastal Conservation*
750 2004; 10: 129-138.

751 Elliott M, Mander L, Mazik K, Simenstad C, Valesini F, Whitfield A, et al. Ecoengineering with
752 Ecohydrology: Successes and failures in estuarine restoration. *Estuarine, Coastal and*
753 *Shelf Science* 2016; 176: 12-35.

754 Environment Agency. Pagham to East Head Coastal Defence Strategy, Worthing, 2007.

755 Erfanzadeh R, Garbutt A, Petillon J, Maelfait JP, Hoffmann M. Factors affecting the success
756 of early salt-marsh colonizers: seed availability rather than site suitability and
757 dispersal traits. *Plant Ecology* 2010; 206: 335-347.

758 Esteves LS. Is managed realignment a sustainable long-term coastal management approach?
759 *Journal of Coastal Research* 2013; Special Issue 65: 933-938.

760 European Parliament and the Council of the European Commission. Council directive
761 92/43/EEC of 21 May 1992 on the conservation of natural habitats and of wild fauna
762 and flora. *Official Journal of the European Communities* 1992; Series L206:
763 22.12.2000.

764 Foster NM, Hudson MD, Bray S, Nicholls RJ. Research, policy and practice for the
765 conservation and sustainable use of intertidal mudflats and saltmarshes in the Solent
766 from 1800 to 2016. *Environmental Science & Policy* 2014; 38: 59-71.

767 French PW. Managed realignment - The developing story of a comparatively new approach
768 to soft engineering. *Estuarine Coastal and Shelf Science* 2006; 67: 409-423.

769 Hazelden J, Boorman LA. Soils and 'managed retreat' in South East England. *Soil Use and*
770 *Management* 2001; 17: 150-154.

771 Howe AJ, Rodriguez JF, Spencer J, MacFarlane GR, Saintilan N. Response of estuarine
772 wetlands to reinstatement of tidal flows. *Marine and Freshwater Research* 2010; 61:
773 702-713.

774 Hvorslev MJ. Subsurface exploration and sampling of soils for civil engineering purposes.
775 Vicksburg, Mississippi: Waterways Experiment Station, 1949.

776 Johnston SG, Keene AF, Bush RT, Burton ED, Sullivan LA, Isaacson L, et al. Iron geochemical
777 zonation in a tidally inundated acid sulfate soil wetland. *Chemical Geology* 2011;
778 280: 257-270.

779 Ketcham RA, Carlson WD. Acquisition, optimization and interpretation of X-ray computed
780 tomographic imagery: applications to the geosciences. *Computers & Geosciences*
781 2001; 27: 381-400.

782 Koretsky CM, Van Cappellen P, DiChristina TJ, Kostka JE, Lowe KL, Moore CM, et al. Salt
783 marsh pore water geochemistry does not correlate with microbial community
784 structure. *Estuarine, Coastal and Shelf Science* 2005; 62: 233-251.

785 Krawiec K. Medmerry, West Sussex, UK: Coastal Evolution from the Neolithic to the
786 Medieval Period and Community Resilience to Environmental Change. *The Historic
787 Environment: Policy & Practice* 2017; 8: 101-112.

788 Luther GW, Church TM. Seasonal cycling of sulfur and iron in porewaters of a Delaware salt-
789 marsh. *Marine Chemistry* 1988; 23: 295-309.

790 Marani M, Silvestri S, Belluco E, Ursino N, Comerlati A, Tosatto O, et al. Spatial organization
791 and ecohydrological interactions in oxygen-limited vegetation ecosystems. *Water
792 Resources Research* 2006; 42.

793 Mazik K, Musk W, Dawes O, Solyanko K, Brown S, Mander L, et al. Managed realignment as
794 compensation for the loss of intertidal mudflat: A short term solution to a long term
795 problem? *Estuarine, Coastal and Shelf Science* 2010; 90: 11-20.

796 Miller H, Croudace IW, Bull JM, Cotterill CJ, Dix JK, Taylor RN. A 500 Year Sediment Lake
797 Record of Anthropogenic and Natural Inputs to Windermere (English Lake District)
798 Using Double-Spike Lead Isotopes, Radiochronology, and Sediment Microanalysis.
799 *Environmental Science & Technology* 2014; 48: 7254-7263.

800 Moller I, Kudella M, Rupprecht F, Spencer T, Paul M, van Wesenbeeck BK, et al. Wave
801 attenuation over coastal salt marshes under storm surge conditions. *Nature
802 Geoscience* 2014; 7: 727-731.

803 Mossman HL, Brown MJH, Davy AJ, Grant A. Constraints on Salt Marsh Development
804 Following Managed Coastal Realignment: Dispersal Limitation or Environmental
805 Tolerance? *Restoration Ecology* 2012; 20: 65-75.

806 Odgaard A. Three-dimensional methods for quantification of cancellous bone architecture.
807 *Bone* 1997; 20: 315-328.

808 Pearce J, Khan S, Lewis P. Medmerry managed realignment—sustainable coastal
809 management to gain multiple benefits. *ICE Coastal Management. Innovative Coastal
810 Zone Management: Sustainable Engineering for a Dynamic Coast.*, Belfast, UK, 2011.

811 Polder G, Hovens H, Zweers A. Measuring shoot length of submerged aquatic plants using
812 graph analysis. *Proceedings of the ImageJ User and Developer Conference 2010,*
813 *Mondorf-les-Bains, Luxembourg, 27-29 October 2010, 2010, pp. 172-177.*

814 Reid MK, Spencer KL. Use of principal components analysis (PCA) on estuarine sediment
815 datasets: The effect of data pre-treatment. *Environmental Pollution* 2009; 157:
816 2275-2281.

817 Rowell DL. *Soil science: Methods & applications.* Harlow, Essex: Longman Scientific &
818 Technical, 1994.

819 Rupprecht F, Moller I, Paul M, Kudella M, Spencer T, van Wesenbeeck BK, et al. Vegetation-
820 wave interactions in salt marshes under storm surge conditions. *Ecological
821 Engineering* 2017; 100: 301-315.

822 Shennan I, Long AJ, Rutherford MM, Green FM, Innes JB, Lloyd JM, et al. Tidal marsh
823 stratigraphy, sea-level change and large earthquakes, i: a 5000 year record in
824 washington, U.S.A. *Quaternary Science Reviews* 1996; 15: 1023-1059.

825 Shennan I, Long AJ, Rutherford MM, Innes JB, Green FM, Walker KJ. Tidal marsh
826 stratigraphy, sea-level change and large earthquakes—ii: Submergence events
827 during the last 3500 years at Netarts Bay, Oregon, USA. *Quaternary Science Reviews*
828 1998; 17: 365-393.

- 829 Spencer KL, Carr SJ, Diggens LM, Tempest JA, Morris MA, Harvey GL. The impact of pre-
830 restoration land-use and disturbance on sediment structure, hydrology and the
831 sediment geochemical environment in restored saltmarshes. *Science of The Total*
832 *Environment* 2017; 587–588: 47-58.
- 833 Spencer KL, Cundy AB, Croudace IW. Heavy metal distribution and early-diagenesis in salt
834 marsh sediments from the Medway Estuary, Kent, UK. *Estuarine Coastal and Shelf*
835 *Science* 2003; 57: 43-54.
- 836 Spencer KL, Cundy AB, Davies-Hearn S, Hughes R, Turner S, MacLeod CL. Physicochemical
837 changes in sediments at Orplands Farm, Essex, UK following 8 years of managed
838 realignment. *Estuarine Coastal and Shelf Science* 2008; 76: 608-619.
- 839 Tempest JA, Harvey GL, Spencer KL. Modified sediments and subsurface hydrology in natural
840 and recreated salt marshes and implications for delivery of ecosystem services.
841 *Hydrological Processes* 2015; 29: 2346-2357.
- 842 Violante A, Barberis E, Pigna M, Boero V. Factors affecting the formation, nature, and
843 properties of iron precipitation products at the soil-root interface. *Journal of Plant*
844 *Nutrition* 2003; 26: 1889-1908.
- 845 Vogel HJ. Morphological determination of pore connectivity as a function of pore size using
846 serial sections. *European Journal of Soil Science* 1997; 48: 365-377.
- 847 Vranken M, Oenema O, Mulder J. Effects of tide range alterations on salt-marsh sediments
848 in the eastern Scheldt, SW Netherlands. *Hydrobiologia* 1990; 195: 13-20.
- 849 Watts CW, Tolhurst TJ, Black KS, Whitmore AP. In situ measurements of erosion shear stress
850 and geotechnical shear strength of the intertidal sediments of the experimental
851 managed realignment scheme at Tollesbury, Essex, UK. *Estuarine Coastal and Shelf*
852 *Science* 2003; 58: 611-620.
- 853 Wilson AM, Evans T, Moore W, Schutte CA, Joye SB, Hughes AH, et al. Groundwater controls
854 ecological zonation of salt marsh macrophytes. *Ecology* 2015; 96: 840-849.
- 855 Wolanski E, Elliott M. *Estuarine Ecohydrology (Second Edition)*. Boston: Elsevier, 2016.
- 856 Zwolsman JJG, Berger GW, Vaneck GTM. Sediment accumulation rates, historical input,
857 postdepositional mobility and retention of major elements and trace-metals in salt-
858 marsh sediments of the Scheldt estuary, SW Netherlands. *Marine Chemistry* 1993;
859 44: 73-94.

860

861

862

**Medmerry Managed
Realignment Site
(West Sussex, United
Kingdom)**

**Orplands Farm Managed
Realignment Site (Essex,
United Kingdom)**

**Natural Saltmarsh
(Hamble estuary,
Hampshire,
United Kingdom)**

Post-site inundation intertidal	Physical properties varied in	Post-site inundation: Poorly consolidated oxic unit with a high abundant root material and omlplex, interconnected pore networks	Layer 1: Thin (mm) oxidised surface layer rich in plant litter
Terrestrial	terrestrial unit but mottled oxic conditions were found throughout suggesting a variable	Terrestrial: Firmer sediment layer, lower in organic and moisture content. Geochemical (lower Fe and Mn concentrations), structural (reduced pore distribution and complexity) and	Layer 2: Mottled oxic zone with evidence of a fluctuating water table, rich in abundant (living) root material
Pre- reclamation intertidal	water table and that vertical solute transfer is not inhibited	hydrological (reduced vertical water flux) evidences suggests reduced solute transfer between units	Layer 3: Black unit with reducing anoxic conditions, increased water content

Graphical Abstract: Schematic comparison of the sub-surface physicochemical properties of the sediment found at the Medmerry Managed Realignment Site (this study), Orplands Farm Managed Realignment Site, U.K. (Spencer et al., 2008; Tempest et al., 2015; Spencer et al., 2017) and a typical natural minerogenic saltmarsh (Cundy and Croudace, 1995). Not drawn to uniform vertical scale.

Figures

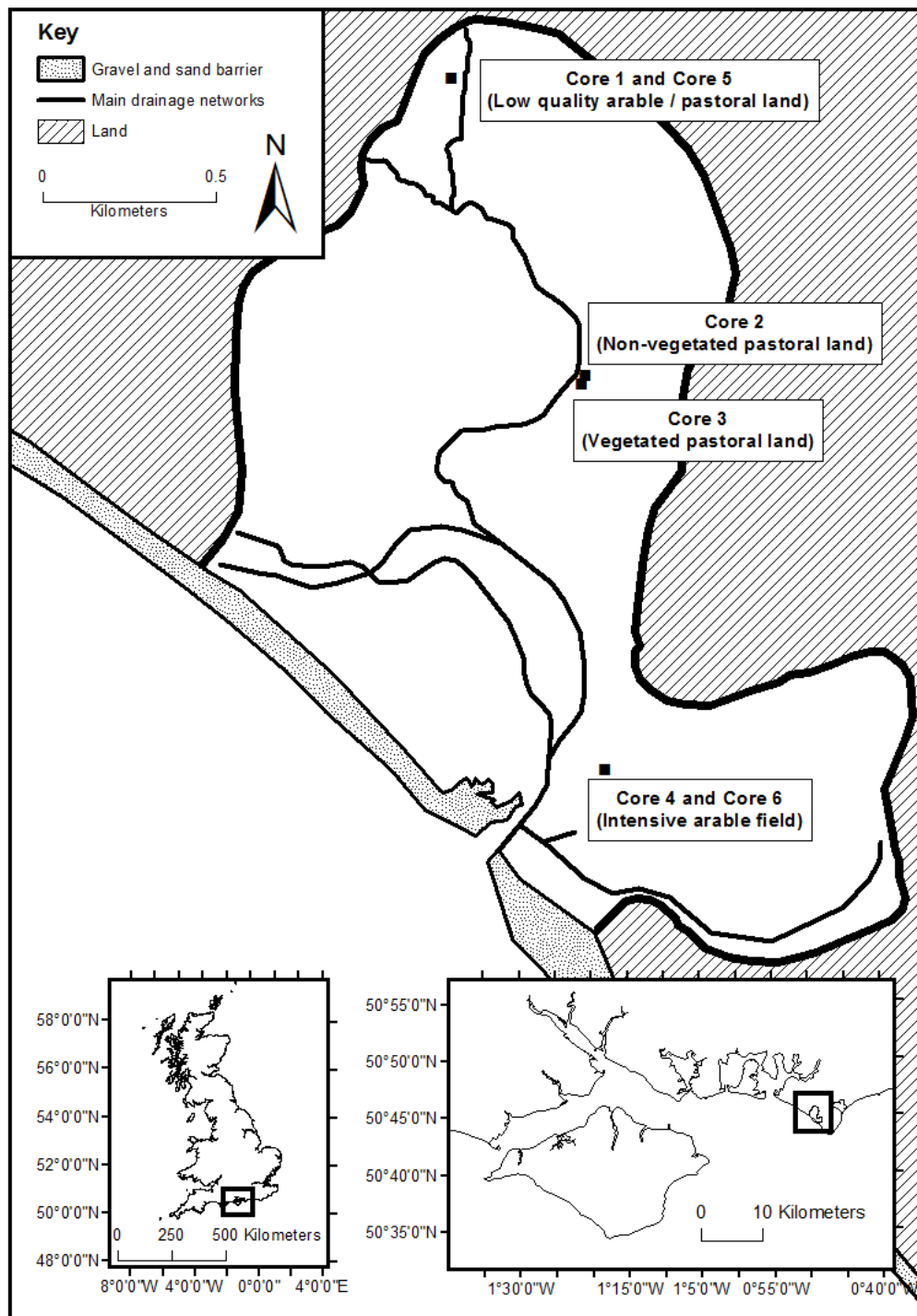


Figure 1: The Medmerry Managed Realignment Site (West Sussex, UK) and wider national (insert, left) and regional (insert, right) location. Coring locations are named and marked with black squares.

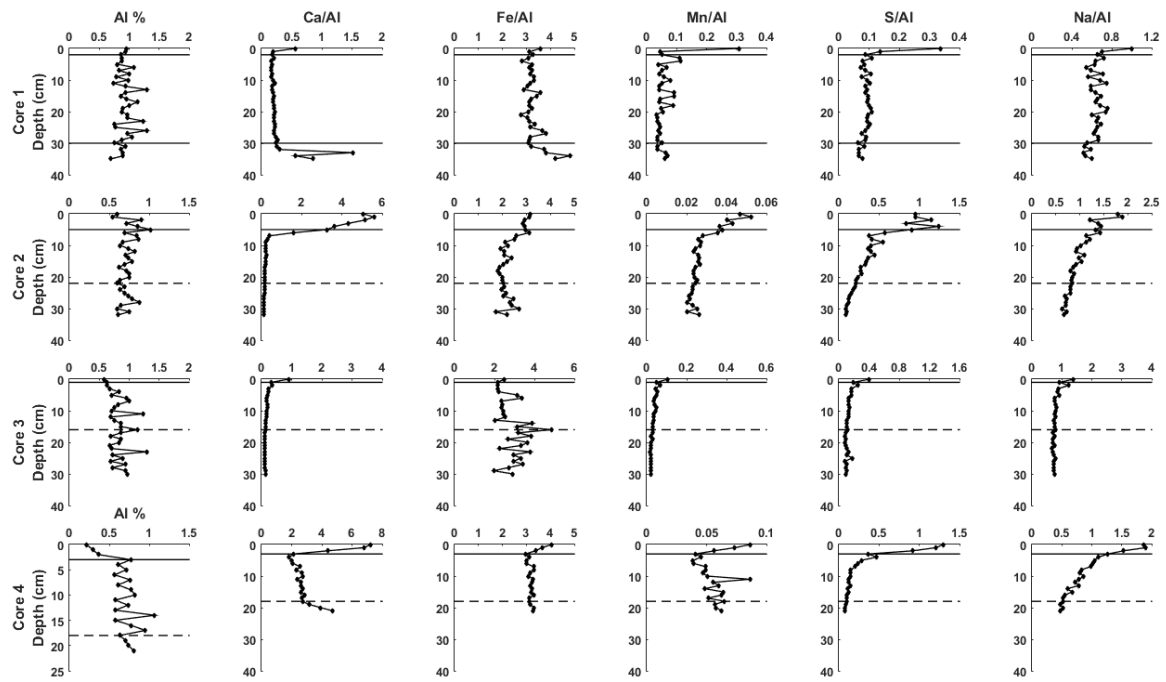


Figure 2: Variations in Al, Ca, Fe, Mn, S and Na concentration with depth from the 2015 core samples.

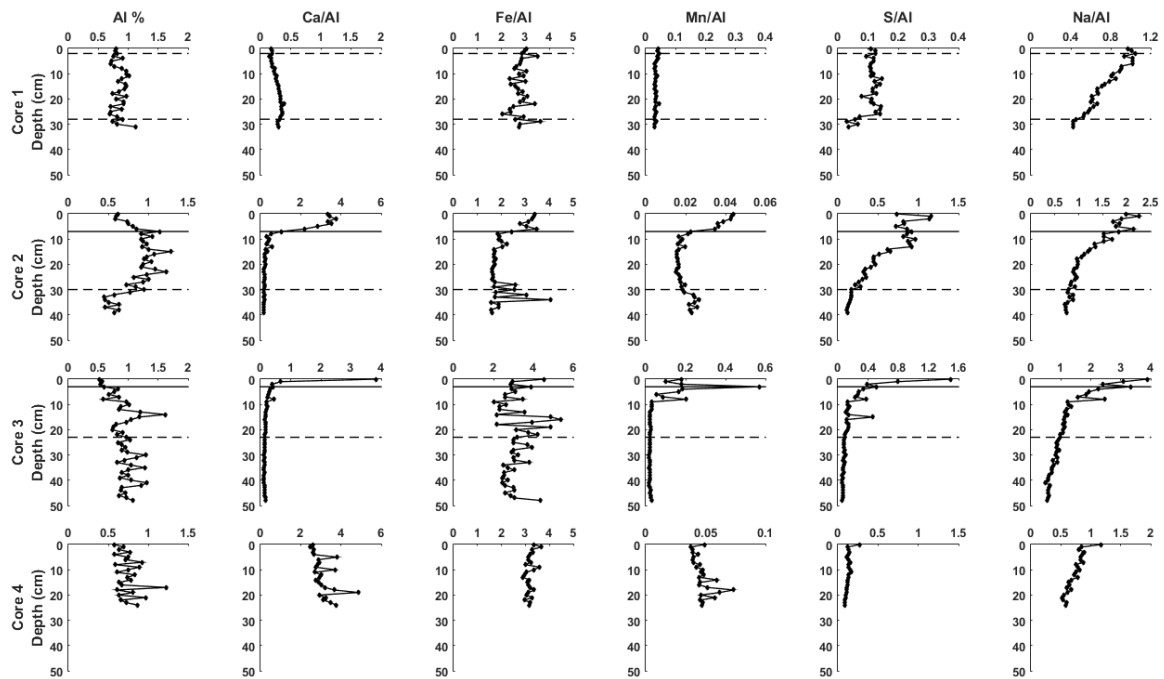


Figure 3: Variations in Al, Ca, Fe, Mn, S and Na concentration with depth from the 2016 core samples.

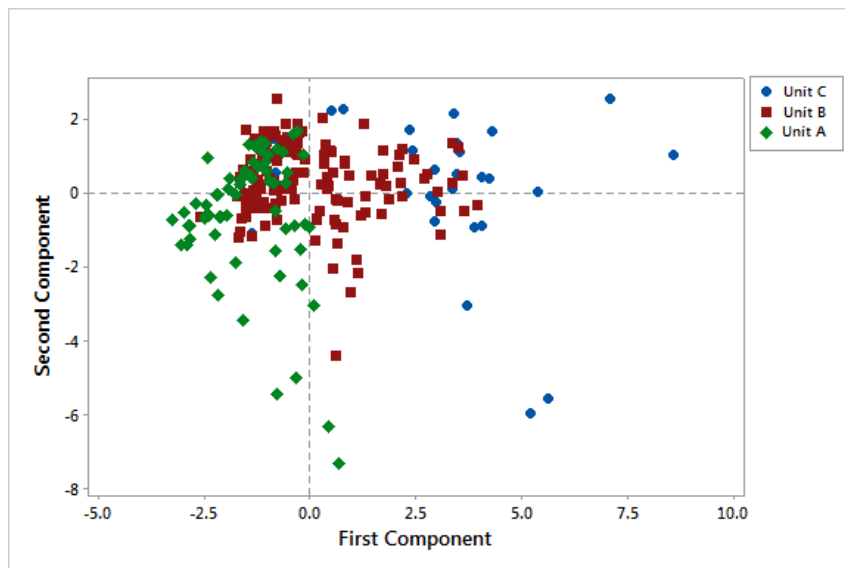


Figure 4: Principle component analysis (PCA) scores for the three sediment units identified in Cores 1 – 4 in 2015 and Cores 1 – 3 in 2016. Components 1 and 2 collectively accounted for 49.6 % of the total variance.

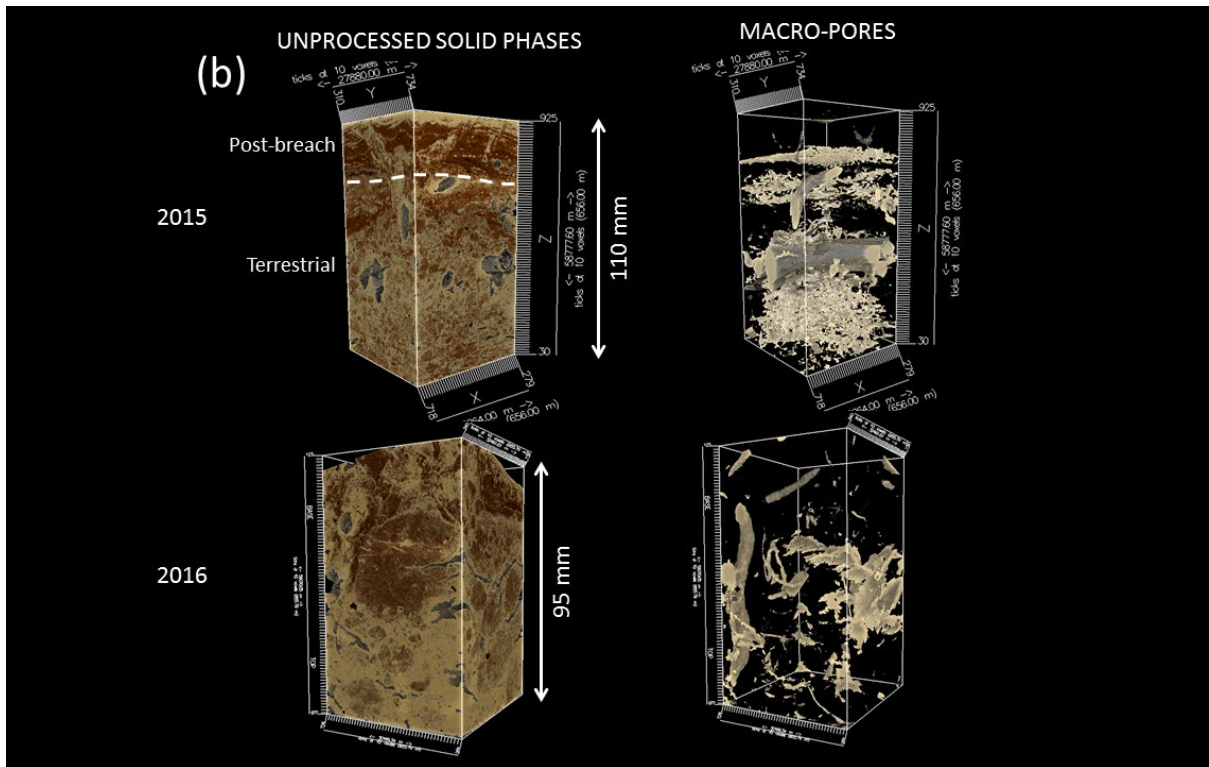
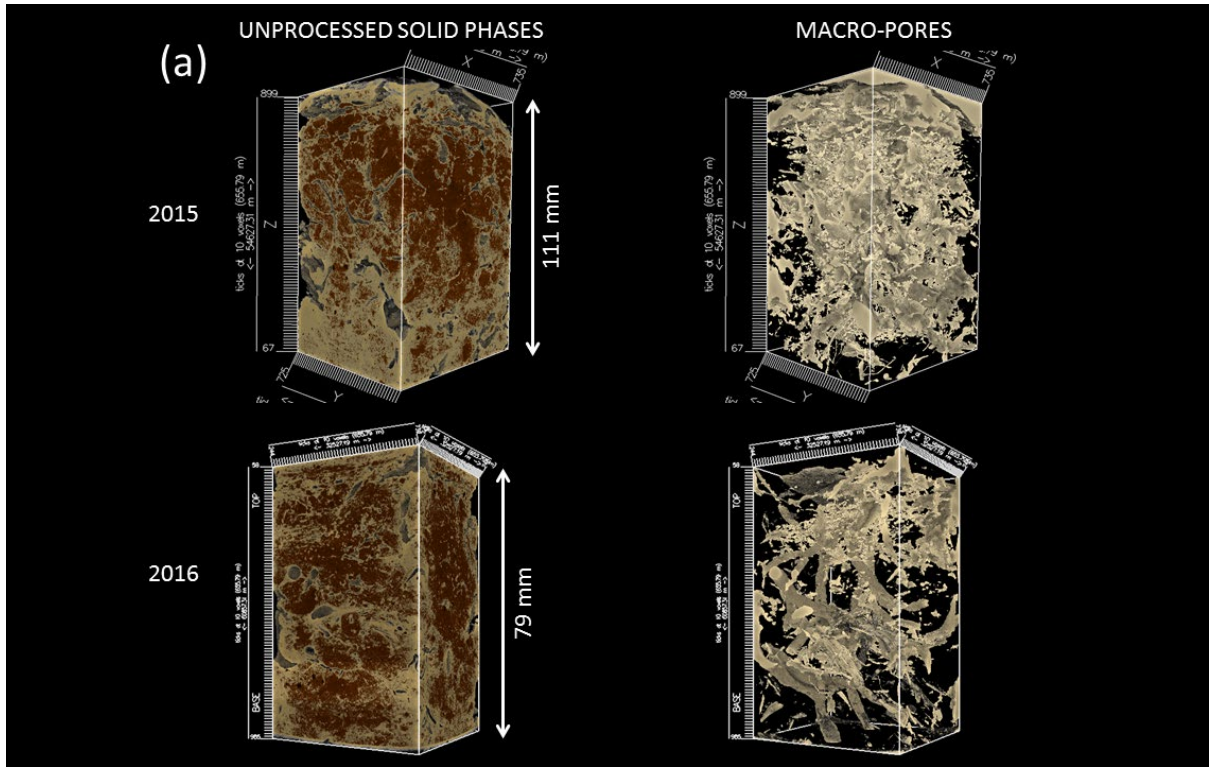


Figure 5: Reconstructions of sediment phases imaged used μ CT analysis in (a) Core 1 and (b) Core 2.

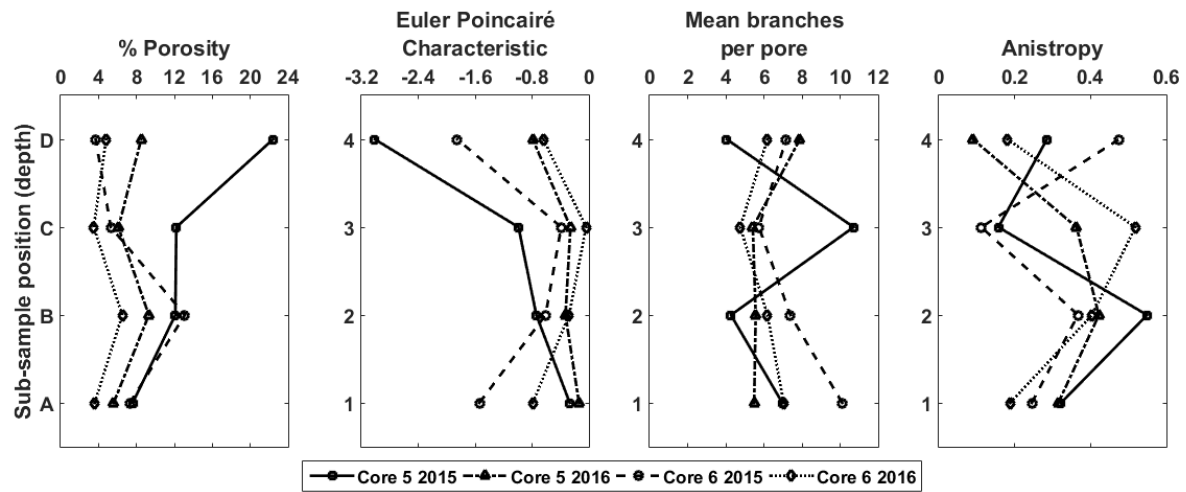
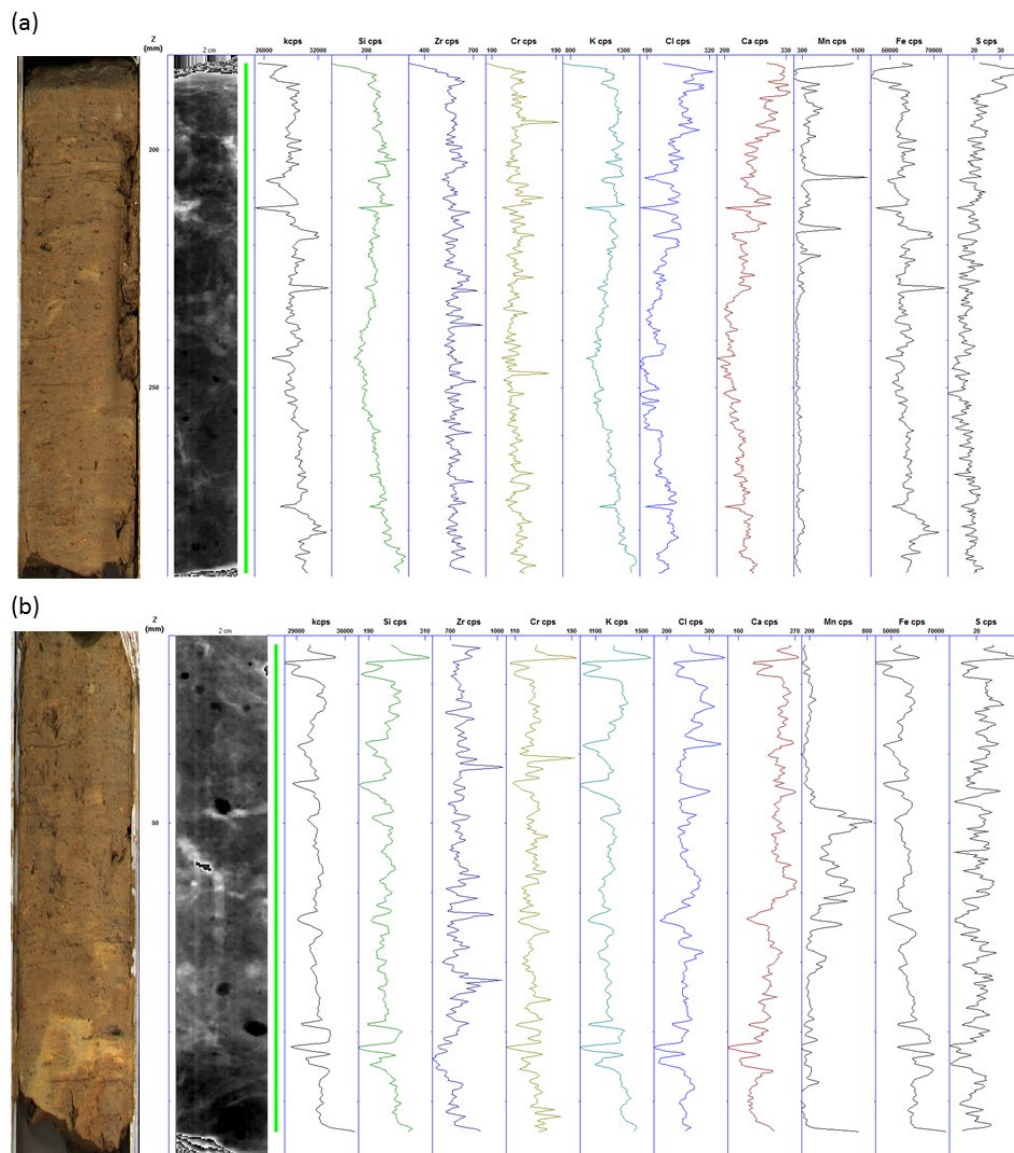


Figure 6: Porosity characteristics for sub-samples of Cores 5 and 6 in 2016 and 2017.



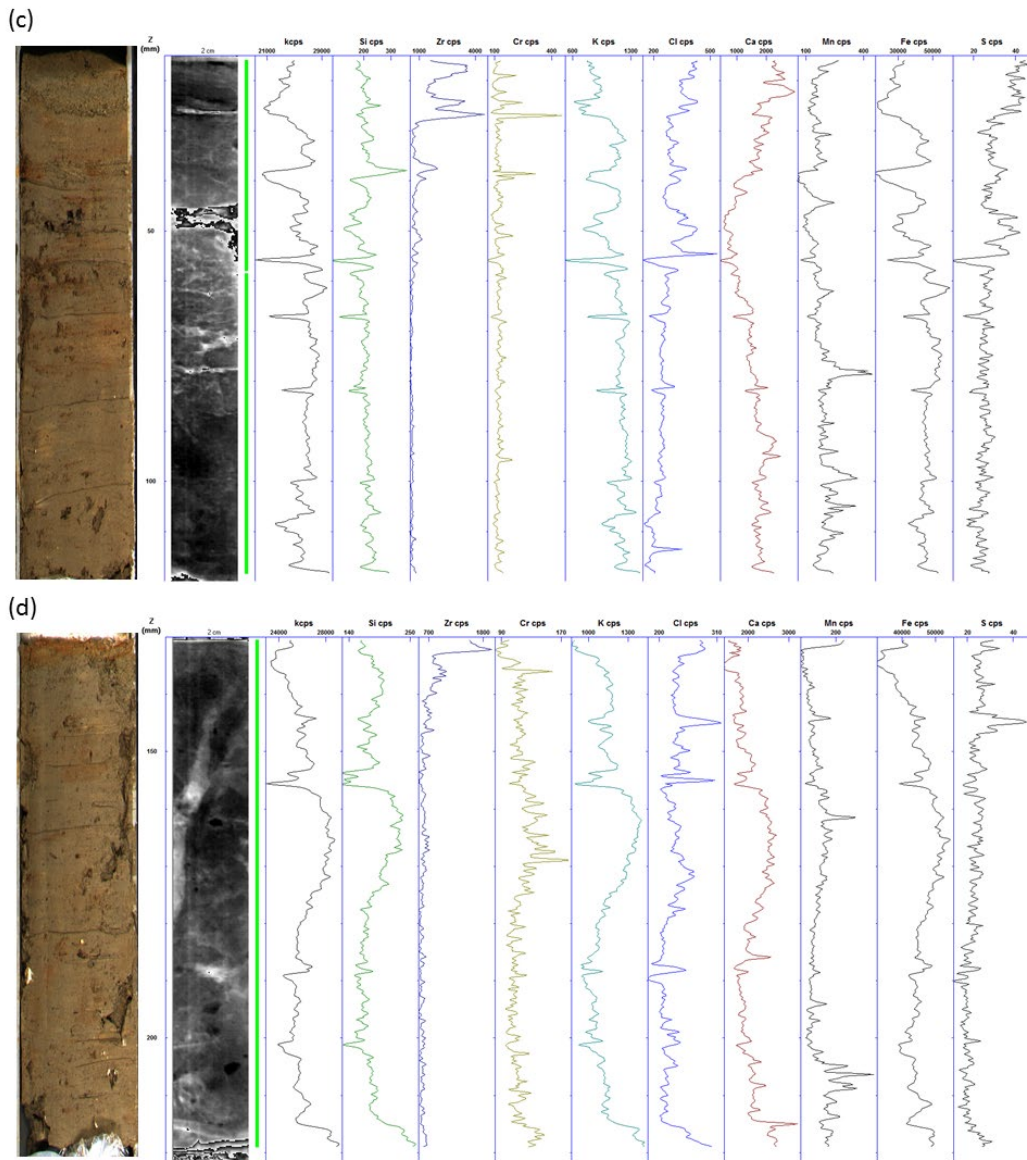


Figure 7: Si, Zr, Cr, K, Cl, Ca, Mn, Fe and S distribution, X-radiograph and photograph of core from (a) Core 5₁₅, (b) Core 5₁₆, (c) Core 6₁₅ and (d) Core 6₁₆. Data are from Itrax scanning: X-axis shows X-ray response, y-axis represents depth.

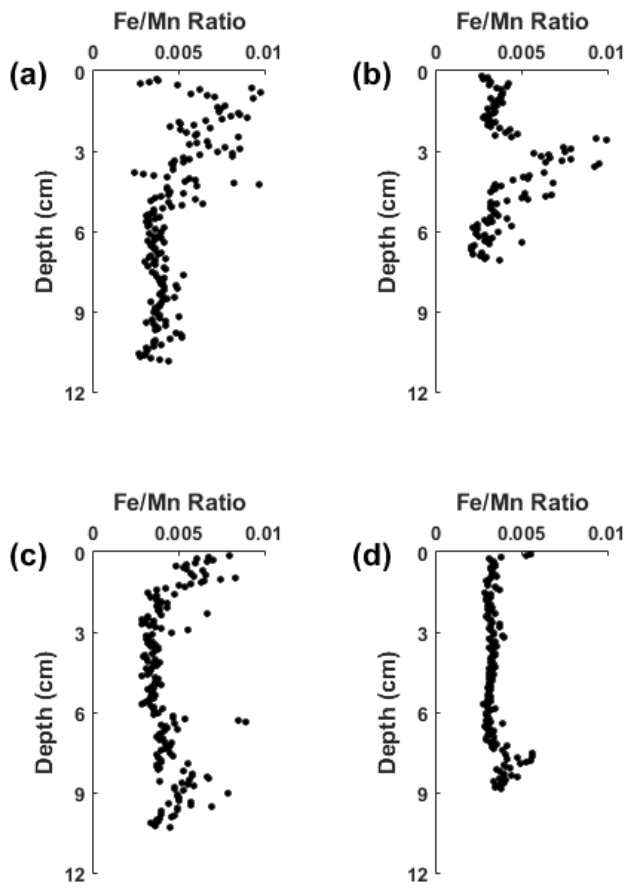


Figure 8: Fe / Mn ratio for (a) Core 5₁₅, (b) Core 5₁₆, (c) Core 6₁₅ and (d) Core 6₁₆ derived from Itrax geochemical data.

Tables

Table 1: Former (terrestrial) land use at sampling locations within the Medmerry Managed Realignment Site and the proposed structural state.

Site	Terrestrial Land Use	Proposed Structure and Composition
Core 1	Low quality arable / pastoral land	Some compaction but interconnected pore networks still expected to be present
Core 2	Non-vegetated pastoral land	Uncompact freely draining sediment
Core 3	Vegetated pastoral land	
Core 4	Intensive arable field	Compact, with low abundance of pore networks resulting lower subsurface solute transfer and anoxic conditions

Table 2: Mean values for physical sediment characteristics for the three sediment units identified (see text for discussion) at the four coring sites (see Figure 1 for locations) in 2015 and 2016.

		Wet Bulk Density		Moisture		Porosity		Loss on		Median Grain		Mud (clay + silt)		
		(kg m ⁻³)		Content (%)				Ignition (%)		Size (µm)		Content (%)		
		Mean	SD	Mean	SD	Mean	SD	Mean	SD	Mean	SD	Mean	SD	
Core 1	2015	Unit C	0.76	0.2	62.22	22.14	0.68	0.11	7.58	0.59	6.58	0.58	97.41	0.68
		Unit B	0.86	0.16	49.04	3.59	0.62	0.07	6.95	2.9	8.44	1.58	94.12	2.52
		Unit A	0.89	0.16	43.99	9.05	0.58	0.09	7.51	2.16	15.34	3.76	92.23	2.95
	2016	Unit C	1.94	0.34	44.82	0.78	0.5	0.09	6.79	11.33	6.03	1.88	89.83	9.77
		Unit B	1.88	0.22	46.42	3.49	0.52	0.06	6.16	5.49	6.71	1.05	87.28	5.25
		Unit A	2.08	0.35	41.84	4.86	0.44	0.11	4.07	3.74	6.19	0.41	91.2	1.45
Core 2	2015	Unit C	0.92	0.23	123.08	14.49	0.72	0.07	5.73	1.83	7.47	0.4	97.67	2.26
		Unit B	1.02	0.38	96.23	21.28	0.65	0.13	9.92	5.87	15.68	8.61	81.44	11.15
		Unit A	1.51	0.45	48.8	6.2	0.33	0.19	7.01	4.72	16.91	5.65	79.48	7.83
	2016	Unit C	1.48	0.27	100.92	5.59	0.72	0.05	4.96	6.15	10.05	2.04	77.36	6.76
		Unit B	1.39	0.33	97.37	29.84	0.73	0.09	12.48	8.54	11.51	7.96	68.23	9.39
		Unit A	1.75	0.3	40.69	8.3	0.53	0.1	4.83	11.1	33.15	25.68	54.1	14.62
Core 3	2015	Unit C	0.64	0.06	122.21	9.46	0.81	0.02	18.61	0.47	6.42	0.78	96.19	3.32
		Unit B	0.99	0.28	69.34	11.05	0.61	0.12	13.48	2.77	6.7	0.77	95.18	2.62
		Unit A	0.93	0.2	51.46	12.19	0.58	0.1	4.52	3.74	5.46	0.59	96.79	5.63
	2016	Unit C	1.39	0.21	118.04	26.02	0.76	0.03	19.21	3.65	11.06	0.86	73.86	3.16
		Unit B	1.71	0.28	69.06	17.39	0.61	0.09	9.88	6.89	7.46	2.46	84.49	7.96
		Unit A	2.18	0.28	40.66	3.64	0.41	0.08	3.24	8.7	7.39	3.25	84.81	9.4
Core 4	2015	Unit C	0.94	0.14	47.95	0.67	0.58	0.07	5.5	15.66	46.48	28.77	59.17	20.19
		Unit B	0.98	0.2	42.25	3.7	0.54	0.1	5.18	3.83	8.54	1.48	89.73	5.13
		Unit A	0.93	0.14	36.89	1.97	0.55	0.07	4.38	1.44	7.52	0.6	92.29	2.33
	2016	Unit C	1.94	0.33	36.62	4.4	0.46	0.09	4.85	8.59	10.2	8.43	78.06	9.93

Table 3: Porosity analysis derived from μ CT analysis divided into sub-samples. Data are presented based on different sediment facies. Core 5 was taken from an area of former lower intensity arable agriculture; Core 6 was taken from an area of former high intensity arable agriculture.

	% Macroporosity	Macro-pore abundance	Pore Connectivity (Euler-Poincaré Characteristic)	Pore network complexity (no. of braches per pore)	Pore Anisotropy
Core 5 2015 A-D	7.6 – 22.4	Low (mean 3672), particularly in the upper sub-sample	-3.01 – -0.27, increasing upwards apart from upper sub-sample	4.05 – 10.71 with no distinctive patterns evident	Moderately high (mean 0.33), although much higher in lower (A and B) sub-samples
Core 5 2016 A-D	5.6 – 6.1	High (mean 5265) although lower in the upper sub-sample	-0.79 – -0.14, increasing upwards apart from upper sub-sample	5.42 – 7.89. Higher in upper sub-sample compared to other three	Moderately high (mean 0.3), but particularly low in upper sub-sample
Core 6 2015 lower facies A-C	5.3 – 13.1	High (mean 5133) and decreasing with depth	-1.54 – 0.39, increasing upwards apart from upper sub-sample	5.74 – 10.11, decreasing upwards.	Moderately low (mean 0.24)
Core 6 2015 upper facies D (post-breach)	3.7	Very high (9458)	-1.85	7.17, greater than the preceding sub-sample	High (0.48)
Core 6 2016 A-D	3.5 – 6.5	Moderately high (mean 4608) and decreasing downwards	-0.79 – -0.04, increasing upwards apart from upper sub-sample	4.76 – 7.04, following same pattern as 2015 sample.	Moderately high (mean 0.32), although lower in upper and lower sub-samples (A and D)